Mosher, D.C., Erbacher, J., and Malone, M.J. (Eds.)
Proceedings of the Ocean Drilling Program, Scientific Results Volume 207

14. Data Report: Log-Adjusted Depth Scales for Cretaceous Black Shale Deposits from Demerara Rise[1]

Matt O'Regan[2]

ABSTRACT

Multiple copies of Cretaceous black shales extending from the early Cenomanian to the end of the Santonian were recovered at five sites on Demerara Rise during Leg 207 of the Ocean Drilling Program. These sediments are primarily composed of laminated organic-rich claystones interbedded with coarser, lightly laminated foraminferal-bearing packstones and wackestones. The black shales represent the local expression of widespread organic-rich sedimentation in the Atlantic during the mid-Cretaceous. However, incomplete recovery prevented construction of continuous composite sections, resulting in uncertainties concerning the correct stratigraphic placement of individual cores. By combining high-resolution measurements of bulk density collected shipboard on the multisensor track with continuous downhole measurements of formation resistivity using the Formation MicroScanner, an equivalent logging depth scale was constructed for black shales recovered from Sites 1258, 1260, and 1261. The integrated depths approach centimeter-scale resolution and are supported by comparisons of coarser resolution natural gamma ray emissions collected on cores and through downhole logging operations. The new depths highlight the extent of both intra- and intercore gaps and provide an opportunity to further constrain temporal and spatial paleoceanographic changes captured in proxy records from these sediments.

[1] O'Regan, M., 2007. Data report: log-adjusted depth scales for Cretaceous black shale deposits from Demerara Rise. *In* Mosher, D.C., Erbacher, J., and Malone, M.J. (Eds.), *Proc. ODP, Sci. Results,* 207: College Station, TX (Ocean Drilling Program), 1–29. doi:10.2973/odp.proc.sr.207.113.2007
[2] Graduate School of Oceanography, University of Rhode Island, Narragansett RI, 02882, USA.
oregan@gso.uri.edu

Initial receipt: 28 March 2006
Acceptance: 13 February 2007
Web publication: 23 April 2007
Ms 207SR-113

INTRODUCTION

A principal objective of Ocean Drilling Program (ODP) Leg 207 was to recover shallowly buried Cretaceous black shale deposits from Demerara Rise that could be used to track paleoceanographic changes in the tropical Atlantic during the early stages of its formation. A total of 650 m of black shales was recovered from depths between 180 and 650 meters below seafloor (mbsf) (Erbacher, Mosher, Malone, et al., 2004). These sediments came from five sites that formed a modern depth transect extending between 1900 and 3200 meters below sea level (mbsl) (Fig. F1). The black shales ranged from Cenomanian through Santonian in age and were characterized by decimeter-scale alternations between organic-rich black shale and laminated foraminiferal packstone with occasional glauconitic bioturbated intervals. These alternations have been interpreted to reflect varying levels of bottom water dysoxia and surface water productivity (Erbacher, Mosher, Malone, et al., 2004).

Drilling through these alternating layers of fissile organic-rich sediments and cemented packstones and wackestones was difficult, and from core to core, recovery through the black shales was extremely variable. Although three holes were drilled at Sites 1257 and 1258 and two holes were drilled at Sites 1260 and 1261, 100% recovery through the black shale sequences was not achieved at any site. Drilling was conducted using the rotary core barrel, and through visual core inspection and depth matching it is apparent that a number of intracore gaps exist. These likely arose from the lithified packstones and wackestones plugging the drill bit, while pumping drill fluid under pressure washed away some of the more fissile organic-rich layers. As a result of the incomplete core recovery, the success of paleoceanographic reconstructions requires that the recovered cores be placed in their correct stratigraphic positions, constraining both the existence and extent of both intra- and intercore gaps.

Geophysical wireline logging offers a continuous downhole record of changing sediment properties that can be correlated with shipboard whole-core measurements performed using the multisensor track (MST). The integration of core and logging data and the development of equivalent logging depths is becoming more routine during ODP legs. However, differences in the resolution between core and logging data often limit the precision of these exercises to a vertical resolution of 10–20 cm. A common practice is to first generate a composite section through centimeter-scale alignment of cores from different holes before integrating the composite section with the logging data to map the meters composite depth (mcd) scale onto an equivalent logging depth (eld) scale, which is sometimes referred to as revised meters composite depth. Integration of the composite section constructed using core data and logging data is a useful way to address elastic expansion of sediments, an inevitable consequence of removing the cores from the in situ stress conditions (MacKillop et al., 1995; Moran, 1997).

During Leg 207, the cyclic nature of the black shales was captured by core and logging measurements of physical properties. The organic-rich layers were characterized as having high porosity and natural radioactivity and low density, compressional wave velocity, magnetic susceptibility, and resistivity (Fig. F2). The competency of the petrophysical signal obviously varies as a function of the instrument resolution. For instance, although natural gamma ray (NGR) emissions are a common way of identifying organic-rich deposits (Rider, 1996), the highest verti-

F1. Location of Demerara Rise, p. 10.

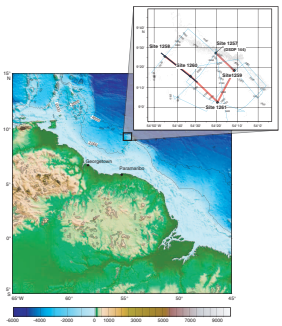

F2. Petrophysical responses through black shales, Hole 1260B, p. 11.

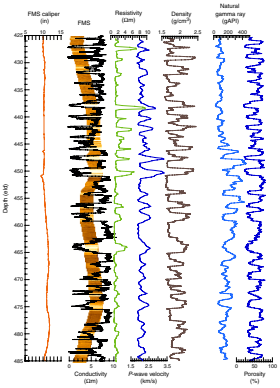

cal resolution for both core and logging NGR instruments are between 10 and 15 cm (Blum, 1997; Goldberg and Meltser, 2001; Shipboard Scientific Party, 2004a). During Leg 207, this resolution tended to blur the contacts and obscure detection of the very high frequency alternations in the black shales. Conversely, formation conductivity, measured with the Formation MicroScanner (FMS) and output at a vertical resolution of 1.27 cm, proved to be an excellent way to track high-frequency lithologic variations. Furthermore, the FMS signal mirrored changes in the MST-derived bulk density with the low-density, high-porosity organic-rich intervals being more conductive than the cemented, high-density, low-porosity packstones and wackestones. This similarity in the response to high-frequency variations allowed integration of the core and logging depths to a higher resolution than that conventionally afforded by integrations performed with coarser resolution tools (Fig. **F3**) Because both resistivity and density vary as a function of porosity, the correspondence between the MST density and the FMS signals has a physical basis that is expressed by the Archie relationship (Archie, 1942):

$$F = a/\phi^m,$$

where

- F = the formation factor (a ratio of the bulk resistivity of a formation to that of the formation fluid),
- a = a constant,
- m = the cementation factor, and
- ϕ = the fractional porosity.

The utility of the high-resolution FMS data in depth matching core and logging data has previously been shown in mapping lithologic changes through carbonate deposits recovered during ODP Leg 166 on the Bahamas Bank slope (Williams and Pirmez, 1999).

Cretaceous shale deposits from three of the five sites (Sites 1258, 1260, and 1261) cored during Leg 207 have been integrated with logging data to develop an eld scale that is used to identify the intra- and intercore gaps. The primary tools for integration were the MST-derived density and the averaged pad data from the FMS tool. However, comparisons with other petrophysical data sets were used to aid in the development of the revised depth scales.

METHODS

Hole-to-hole correlations between cores were made using the software application Splicer, and core-log integration was performed using the software application Sagan. These are both custom-built UNIX platform packages developed by the Lamont-Doherty Earth Observatory Borehole Research Group (LDEO-BRG) and are available through **www.ldeo.columbia.edu/BRG/ODP**. Modifications to these packages were made by H. Pälike (National Oceanographic Center, Southampton, UK), which allowed them to be run on Mac OSX 10.3.

In ODP, core depths are measured by the amount of deployed drill string and recorded by the drillers in mbsf depth scale. When recovery is incomplete, the recovered core is hung from the top of the drilled interval. This represents the most common way of introducing errors into

F3. Hole 1260B FMS conductivity vs. depth-matched MST density, p. 12.

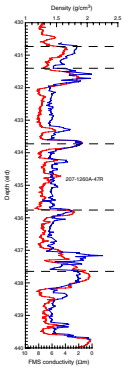

the mbsf depth scale. Other sources of error include (1) recovery >100%, which can result in overlap of the mbsf scale between cores; (2) vertical displacement of the coring tool resulting from ship heave; (3) elastic effects of core expansion; (4) recoring of intervals; or (5) gaps between cores that arise from washing away sediments.

Splicer allows the user to import data sets from multiple holes, and using an interactive cross-correlation function, align similar features between cores. The depth scale of the realigned cores is termed the mcd scale, and is output as a new column appended to the original data files when correlations are complete. Once core data from multiple holes are aligned, Splicer can be used to generate a composite section that is constructed by selecting the highest quality intervals of recovered material. Where all material within a given sequence has been successfully recovered from multiple holes, the composite section represents a continuous stratigraphic record. Because Splicer does not allow for expansion or compression of material within an individual core, this procedure must be done using Sagan. Sagan allows the user to import core measurements and align them to logging data. Functionally similar to Splicer, an automated cross-correlation function allows the user to align similar features found in the core data with those recorded in the continuous logs and adjust the depths of the cores appropriately. The log-adjusted depths (eld) are then appended to the original data files.

Generally, it is the spliced record that is integrated with the logging data; however, Sagan allows the user to input core data from multiple holes using either the mbsf or mcd depth scales. Although the composite depth scale constructed shipboard was used as a guideline in integrating core and logging depths, mcd scales were not translated directly into equivalent logging depth. Core data were imported into Sagan using the mbsf scale and aligned to the logging data. An iterative process was used, with coring data being passed between Splicer and Sagan until optimal alignment between cores from separate holes and the logging data was achieved. Therefore, no modifications have been made to the shipboard mcd tables; instead, meters below seafloor is directly mapped into equivalent logging depth and a composite section is built for each of the sites by importing the eld depths into Splicer (Fig. F4).

Tools used for correlating core and logging data through the black shales included visual core descriptions, digital core images, and whole-core MST measurements of density, magnetic susceptibility, and NGR emissions, as well as downhole logging data from the FMS tool, the Scintillation Gamma Ray Tool (SGT), and to a lesser extent, the Hostile Environment Litho-Density Sonde and the Accelerator Porosity Sonde. During Leg 207, MST measurements of density, magnetic susceptibility, and NGR were made every 2.5, 2.5, and 7.5 cm, respectively. At Sites 1258, 1260, and 1261, FMS and SGT data were collected on a single tool string (FMS-sonic) and recorded on two separate passes (Shipboard Scientific Party, 2004a).

Three wireline logging tools are commonly employed for collecting NGR measurements during ODP expeditions: the Hostile Environment Gamma Ray Sonde (HNGS) that is commonly run on the triple combo tool string, the third party Multisensor Spectral Gamma Ray Tool (MGT) developed by LDEO-BRG and often run at the top of the triple combo tool string, and the SGT run on the FMS-sonic tool string. The MGT records the highest resolution measurements, followed by the SGT and HNGS, respectively (Fig. F5). During Leg 207, all three tools were run at each of the logged sites. For core-log correlation, the SGT data were used as they (1) provided comparable resolution to the MGT

F4. Process used to integrate the core and log data, p. 13.

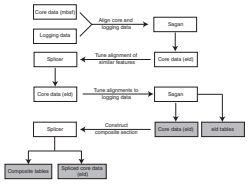

F5. Comparison of HNGS, MGT, and SGT from the black shales, Site 1260, p. 14.

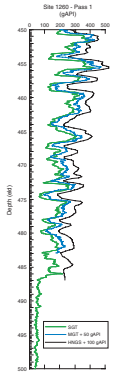

(Fig. F5), (2) the tool was positioned lower on the logging tool string than the MGT, thus collecting data further into the borehole, and (3) the data were collected on the same tool string as the FMS data, the primary tool for core-log integration.

Depth matching between the passes was performed shipboard by the logging staff scientist. The wireline heave compensator was used during logging and recorded between 1.3 and 2 m of heave at Sites 1258 and 1260, but during two occasions at Site 1261, the maximum heave of 3 m was exceeded (Shipboard Scientific Party, 2004b, 2004c, 2004d). Depth matching between passes corrected for much of this heave-generated tool string movement during logging; however, offsets between passes remained through certain intervals, and for each site a single pass was selected as the arbitrary depth scale to which the core data were aligned.

The FMS tool is equipped with four orthogonal pads, each outfitted with 16 button electrodes that record formation resistivity when in contact with the borehole wall. Processing FMS data produces spatially orientated high-resolution images of formation resistivity. These images are commonly used as the end product of the FMS tool. For core-log integration of the black shales, LDEO-BRG extracted the raw average uncalibrated formation conductivity from each of the four pads. These data were averaged to give a single formation conductivity value having a vertical resolution of 1.27 cm. The quality of all logging data through the black shales was excellent, with little borehole diameter variation (see Shipboard Scientific Party, 2004b, 2004c, and 2004d for more detailed discussions of log quality).

RESULTS AND DISCUSSION

The ties used to match the coring data with the logging table are presented in Table T1. Where multiple ties exist for a single core, the mbsf depth between the two tie points had to be stretched or compressed. A large number of the tie points require that a stretching factor be applied. This is counterintuitive, as the core depth is more commonly compressed to account for elastic rebound from stress relief. The stretching required to match the core and log data indicates (1) the prevalence of intracore gaps where portions of lithified and/or organic-rich material were lost due to drilling disturbances and/or (2) the pore pressures through the black shales were significantly higher than hydrostatic, so that the removal of these samples from depth did not translate into significant stress relief.

T1. Tie points used to correlate core depth scale with logging scale, p. 24.

At all sites, significant differences exist between the drillers depth to seafloor and the loggers depth to seafloor (Table T2) (Shipboard Scientific Party, 2004b, 2004c, 2004d). The loggers depth to seafloor is determined by monitoring the amount of cable released from the logging winch (with the seafloor identified by a spike in the NGR profile), whereas the drillers depth is determined by counting the number of pipe stands deployed. The discrepancy between these depths was not resolved shipboard and continues to be problematic. The offsets are likely a result of measurement error in either the drillers or loggers depth to seafloor, and not an artifact of tidal action.

T2. Reported depths to seafloor, p. 26.

Site 1258

Site 1258 was the most challenging of the three sites to integrate. Not only was it the only site where three holes were drilled, but during coring in Hole 1258C, a 5-m advance was used in an attempt to increase core recovery, thereby increasing the number of cores and reducing the potential length of continuous sequences. An 8-m offset existed between the wireline depth to seafloor (3195 meters below rig floor [mbrf]) and the drillers depth to seafloor (3203 mbrf) (Shipboard Scientific Party, 2004b). Faulting or slumping in the Eocene sequence of Hole 1258A resulted in 22 m of missing material when compared to Holes 1258B and 1258C. This missing interval was recorded in the shipboard mcd data and explains the large differences in the offsets of cores from different holes in Table **T1.** Core data at Site 1258 were aligned with pass 2 of the FMS tool. Aligned cores include Cores 207-1258A-40R to 50R, 207-1258B-44R to 57R, and 207-1258C-14 to 31R.

Logging was performed at the end of coring operations in Hole 1258C. The recovered transition into the black shales is marked by a sharp unconformity in Cores 207-1258B-44R and 207-1258C-15R that was not captured in Hole 1258A. The first definitive tie point among all three holes occurs in a visually distinct carbonate-enriched interval that is cut by a 3-cm band of black organic-rich material. The interval is present in Samples 207-1258A-42R-5, 60–100 cm, 207-1258B-45R-3, 83–120 cm, and 207-1258C-16R-2, 68–110 cm, and appears as a broad increase in density and a broad low in smoothed susceptibility and lies just above a prominent spike in the NGR records in each of the cores (Fig. **F6**). The top of this interval is assigned to a depth of 402.92 eld. By placing the tie point at this level, the top of Core 207-1258A-42R (which is exclusively composed of laminated calcareous claystone with organic carbon) extends roughly 3 m above the logged transition in Hole 1258C, and thus represents an expanded sequence not recovered in Hole 1258C. Similarly, in Hole 1258B the upper 1.5 m of black shale in Core 207-1258B-44R has been described as a debris flow and was not recovered in Hole 1258C (Shipboard Scientific Party, 2004b). The transition into the black shales in the three holes of Site 1258 is not synchronous (Fig. **F6**). To account for this, in equivalent logging depth, the uppermost 3 m of Core 207-1258A-42R sits above the transition into the black shales as identified in the logging data, whereas the bottom of Core 207-1258B-44R and the top of Core 207-1258B-45R are forced to overlap to account for the extra 1.5 m of the debris flow.

Alignments of individual cores with the logging data are illustrated in Figure **F7A** and **F7B,** and the composite section and tie points between the cores are given in Table **T3** and illustrated in Figure **F7C** and **F7D.** Taking the range of black shale deposits to extend from the first tie point in Table **T1** (398.49 eld) to the base of the NGR spike in Section 207-1258B-57R-3, 50 cm (458.75 eld), recovery was 93% through this interval.

Site 1260

Only two holes were drilled at Site 1260. Cores 207-1260A-42R through 52R and 207-1260B-30R through 45R have been aligned with the logging data. Results from the core-log integration are presented in Figure **F8.** Logging was performed in Hole 1260B with a 7-m offset between the loggers (2553 mbrf) and drillers (2560 mbrf) depth to the seafloor (Shipboard Scientific Party, 2004c). Results from the two passes of

F6. Depth-matched log and core data from the black shales, Site 1258, p. 15.

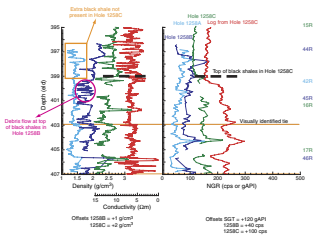

F7. Log-integrated depths for MST density, Site 1258, p. 16.

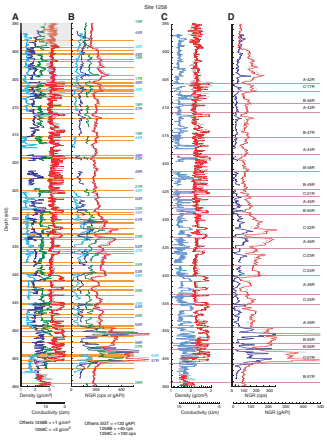

T3. Composite section tie points for Site 1258 log-adjusted coring data, p. 27.

F8. Log-integrated depths for MST density, Site 1260, p. 18.

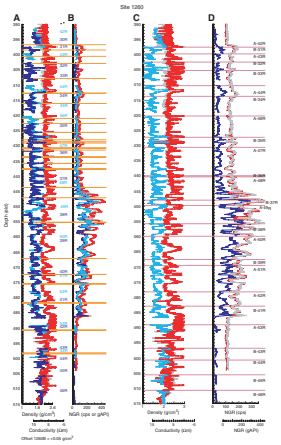

the FMS are very similar, and pass 1 was arbitrarily selected as the basis for depth matching the core and logging data.

The transition into the black shale sequence appears to be captured in Section 207-1260A-42R-CC, 7.5 cm, but is not recovered in Hole 1260B. No tie point exists at this depth because no whole-core measurements were made on core catchers using the MST. However, the glauconitic-rich claystones overlying the black shales in Core 207-1260B-30R can be tied using the smoothed susceptibility data to Core 207-1260A-42R. The transition into the black shales is marked by a rise in NGR emissions and mirrored by a gradual increase in the MST measurements of susceptibility and density and decrease in the FMS. The first tie point is at 396.50 eld and crosses Sections 207-1260A-42R-4, 35 cm, and 207-1260B-30R-3, 73 cm. The top of the black shales occurs at 397.52 eld (Fig. **F9**). The end of the black shale sequence (defined as the top of the synrift Albian sediments) occurs near a transition into very high frequency alternations of claystones and sandstones that have a low NGR signature. This transition occurs at the base of Section 207-1260B-40R-3, 105 cm, at 486.50 eld. Because of the high recovery through Site 1260, a near-continuous composite profile could be spliced together (Table **T4**) and is illustrated in Figures **F8C** and **F8D.** From the first tie point to the approximate top of the Albian-age sediments, 95.5% recovery was achieved.

F9. Depth-matched log and core data from the black shales, Site 1260, p. 20.

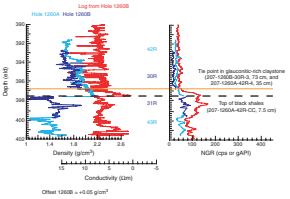

T4. Composite section tie points for Site 1260 log-adjusted coring data, p. 28.

Site 1261

For depth correlation of Site 1261, FMS data from pass 1 were selected as the reference scale. Cores 207-1261A-41R through 51R and 207-1261B-5R through 15R were integrated with the logging data. Results are presented in Figure **F10.** A 12.1-m offset between the core and log depths originates from a difference in the wireline depth to seafloor of 1899 mbrf and the drillers depth to seafloor of 1911.1 mbrf (Shipboard Scientific Party, 2004d). Differences between pass 1 and pass 2 FMS data are minimal above 638 eld. Below 638 eld, an abrupt offset in the FMS data of pass 2 corresponds to an apparent drop in the resolution of the tool. This resolution loss in pass 2 is the primary reason for adopting pass 1 as the absolute depth scale.

Shipboard, a large shift in the NGR emissions measured with the SGT that begins at a depth of 573.85 eld was used to identify the top of the black shales. The equivalent rise in the MST-measured NGR data occurs in Section 207-1261B-5R-4, 15 cm. However, from visual core descriptions, this is above a sharp lithologic boundary separating the overlying glauconite-rich claystones and the underlying black shale sequence. This sharp transition in interval 207-1261B-5R-4, 110–115 cm, is tied to the logs at 574.47 eld (Fig. **F11**). The transition is represented as a drop in density and in the FMS data as a shift into a less variable signal. This transition is missing in Hole 1261A; however, it is possible to tie the interval between Sections 207-1261A-40R-4, 80 cm, and 40R-6, 45 cm, to Sections 207-1261B-5R-1, 5 cm, through 5R-2, 82.5 cm, based upon excellent agreement in the whole-core measurements of MS (magnetic susceptibility), NGR, and GRA (gamma ray attenuation bulk density). This interval lies above the transition into the black shales. Below the transition, a visual match can be made between discrete horizons of dark, organic-rich layers in Sections 207-1261A-41R-2, 40 cm, 72 cm, and 127.5 cm, that correspond to horizons in Sections 207-1261B-5R-6, 75 cm, and 108 cm, and 5R-7, 15 cm. Although it is possible to align these features using MST data, poor core quality in Core 207-1261B-5R

F10. Log-integrated depths for MST density, Site 1261, p. 21.

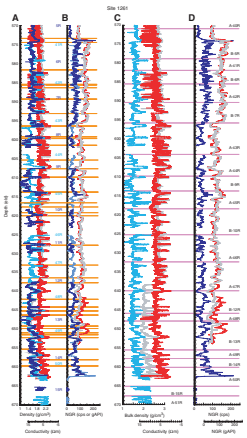

F11. Depth-matched log and core data from the black shales, Site 1261, p. 23.

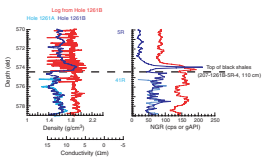

reduces the signal-to-noise ratio and weakens the strength of the density correlation.

Only the FMS data capture the bottom of the black shale sequence in Hole 1261B, as this was the lowest tool on the FMS-sonic tool string (Shipboard Scientific Party, 2004d). The base of the sequence (top of Albian-age sediments) aligns with the base of Core 207-1261B-14R and crosses Core 207-1261A-50R and falls at 662.4 eld. Using the eld depth scales and the revised spliced record, recovery from the first tie point to the approximate top of the Albian deposits was 94% (see Table T5).

T5. Composite section tie points for Site 1261 log-adjusted coring data, p. 29.

SUMMARY

Alignment of the core data with the logging data not only facilitates the correct stratigraphic placement of cores with respect to one another and allows the magnitude of inter- and intracore gaps to be defined, but it also allows data on the age of the sediments to be mapped onto a continuous stratigraphic record. Incorporation of more detailed biostratigraphic and isotopic age markers will further constrain lithologic variation through time and provide a basis for future cyclostratigraphic analyses of the logging data. The differences between the loggers and drillers depth to seafloor at all the studied sites remains unresolved. Integration of the eld scale with other sections of sediment from Sites 1258, 1260, and 1261 must address this discrepancy.

ACKNOWLEDGMENTS

This research used samples and/or data provided by the Ocean Drilling Program (ODP). ODP is sponsored by the U.S. National Science Foundation (NSF) and participating countries under management of Joint Oceanographic Institutions (JOI), Inc. Funding for this research was provided by the U.S. Science Support Program of JOI.

REFERENCES

Archie, G.E., 1942. The electrical resistivity log as an aid in determining some reservoir characteristics. *Trans. Am. Inst. Min., Metall. Pet. Eng.,* 146:54–62.

Blum, P., 1997. Physical properties handbook: a guide to the shipboard measurement of physical properties of deep-sea cores. *ODP Tech. Note,* 26 [Online]. Available from World Wide Web: <**http://www-odp.tamu.edu/publications/tnotes/tn26/INDEX.HTM**>.

Erbacher, J., Mosher, D.C., Malone, M.J., et al., 2004. *Proc. ODP, Init. Repts.,* 207: College Station, TX (Ocean Drilling Program). **doi:10.2973/odp.proc.ir.207.2004**

Goldberg, D., and Meltser, A., 2001. High vertical resolution spectral gamma ray logging: a new tool development and field test results. *Trans. SPWLA Annu. Logging Symp.,* 42:JJ1–JJ13. (Abstract)

MacKillop, A.K., Moran, K., Jarrett, K., Farrell, J., and Murray, D., 1995. Consolidation properties of equatorial Pacific Ocean sediments and their relationship to stress history and offsets in the Leg 138 composite depth sections. *In* Pisias, N.G., Mayer, L.A., Janecek, T.R., Palmer-Julson, A., and van Andel, T.H. (Eds.), *Proc. ODP, Sci. Results,* 138: College Station, TX (Ocean Drilling Program), 357–369. **doi:10.2973/odp.proc.sr.138.118.1995**

Moran, K., 1997. Elastic property corrections applied to Leg 154 sediment, Ceara Rise. *In* Shackleton, N.J., Curry, W.B., Richter, C., and Bralower, T.J. (Eds.), *Proc. ODP, Sci. Results,* 154: College Station, TX (Ocean Drilling Program), 151–155. **doi:10.2973/odp.proc.sr.154.132.1997**

Rider, M.H., 1996. *The Geological Interpretation of Well Logs* (2nd ed.): Caithness (Whittles Publishing).

Shipboard Scientific Party, 2004a. Explanatory notes. *In* Erbacher, J., Mosher, D.C., Malone, M.J., et al., *Proc. ODP, Init. Repts.,* 207: College Station, TX (Ocean Drilling Program), 1–94. **doi:10.2973/odp.proc.ir.207.102.2004**

Shipboard Scientific Party, 2004b. Site 1258. *In* Erbacher, J., Mosher, D.C., Malone, M.J., et al., *Proc. ODP, Init. Repts.,* 207: College Station, TX (Ocean Drilling Program), 1–117. **doi:10.2973/odp.proc.ir.207.105.2004**

Shipboard Scientific Party, 2004c. Site 1260. *In* Erbacher, J., Mosher, D.C., Malone, M.J., et al., *Proc. ODP, Init. Repts.,* 207: College Station, TX (Ocean Drilling Program), 1–113. **doi:10.2973/odp.proc.ir.207.107.2004**

Shipboard Scientific Party, 2004d. Site 1261. *In* Erbacher, J., Mosher, D.C., Malone, M.J., et al., *Proc. ODP, Init. Repts.,* 207: College Station, TX (Ocean Drilling Program), 1–103. **doi:10.2973/odp.proc.ir.207.108.2004**

Williams, T., and Pirmez, C., 1999. FMS images from carbonates of the Bahama bank slope, ODP Leg 166: lithological identification and cyclostratigraphy. *In* Lovell, M.A., Williamson, G., and Harvey, P.K. (Eds.), *Borehole Imaging: Application and Case Histories*. Geol. Soc. Spec. Publ., 159:227–238.

Figure F1. Location of Demerara Rise in the eastern tropical Atlantic. Inset illustrates site map of ODP Leg 207 (from Shipboard Scientific Party, 2004a). Sites 1261, 1260, and 1258 form a modern-day depth transect extending from 1900 to 3200 mbsl. DSDP = Deep Sea Drilling Project.

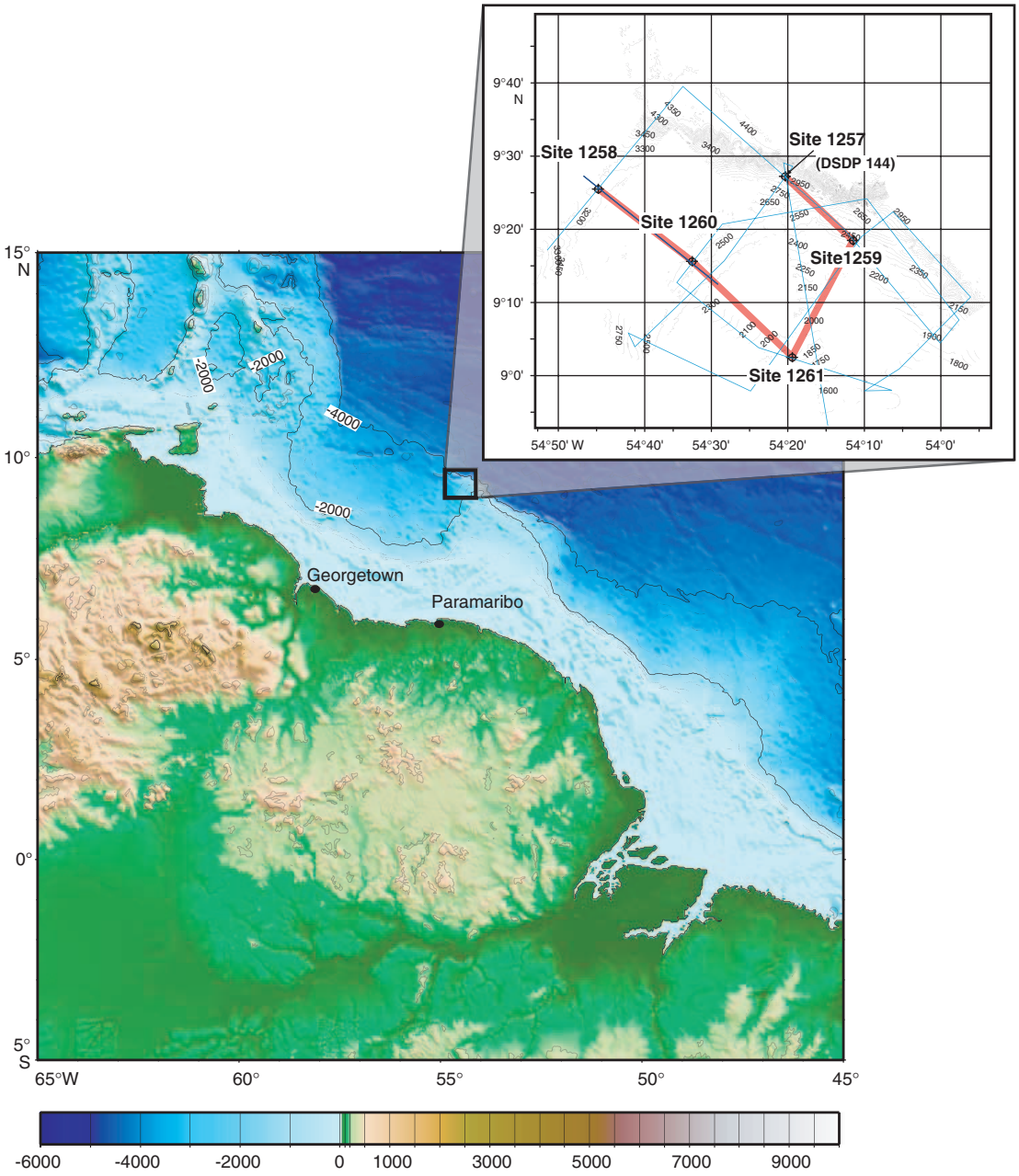

Figure F2. Summary of petrophysical responses through a 60-m interval of black shales in Hole 1260B. Caliper data from the Formation MicroScanner (FMS) tool illustrate relatively constant borehole diameter. The FMS static normalized image forms a backdrop for pad averaged conductivity values from the tool highlighting the highly resistive lithified and cemented intervals (white intervals in static normalized image). The shallow resistivity, *P*-wave velocity, and bulk density all increase across the lithified intervals, whereas NGR and porosity are higher in the organic-rich intervals (darker bands on the FMS static normalized image). eld = equivalent logging depth. gAPI = American Petroleum Institute gamma ray units.

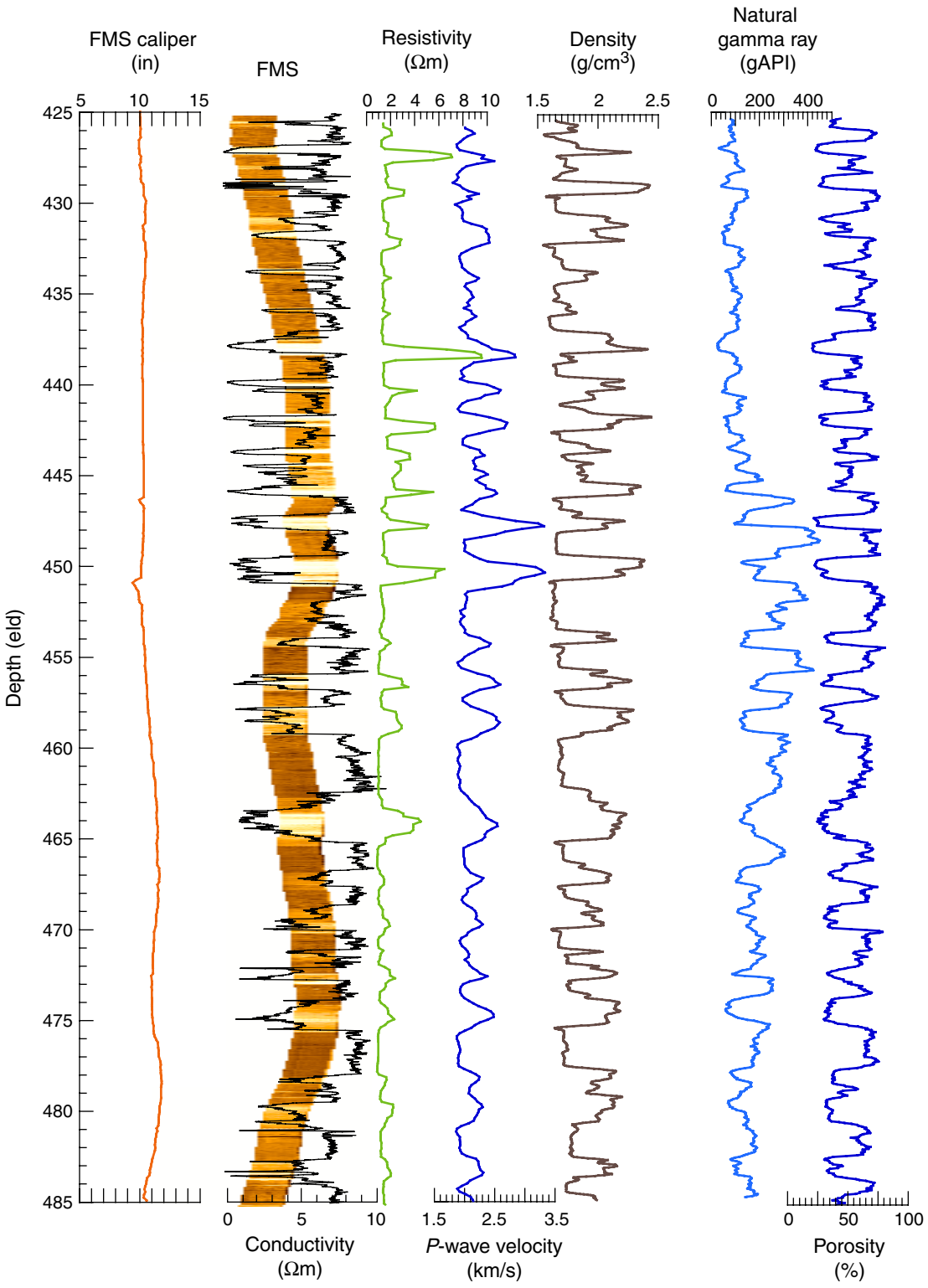

Figure F3. Comparison of Formation MicroScanner (FMS) averaged button data (conductivity) from pass 1 of Hole 1260B and the depth-matched MST density data from Core 207-1260A-47R. No smoothing has been applied to the records, which illustrate the similarity in high-frequency variability between these two data sets. Tie points used in depth matching are marked by black dashed lines. eld = equivalent logging depth.

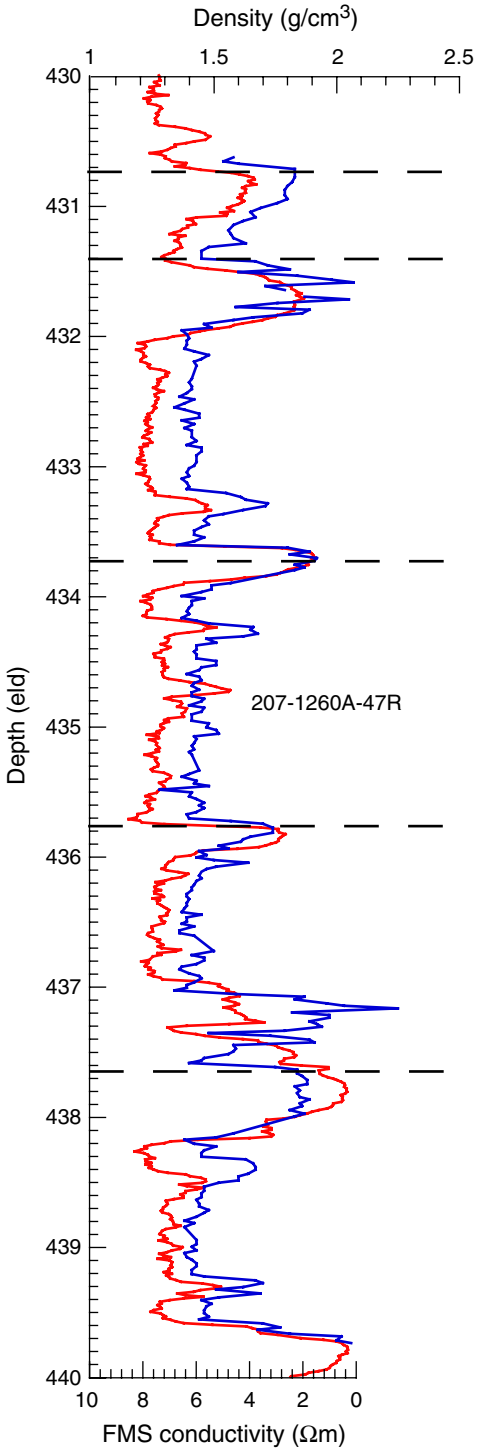

Figure F4. Flow chart outlining process used to integrate the core and log data. mbsf = meters below seafloor. eld = equivalent logging depth.

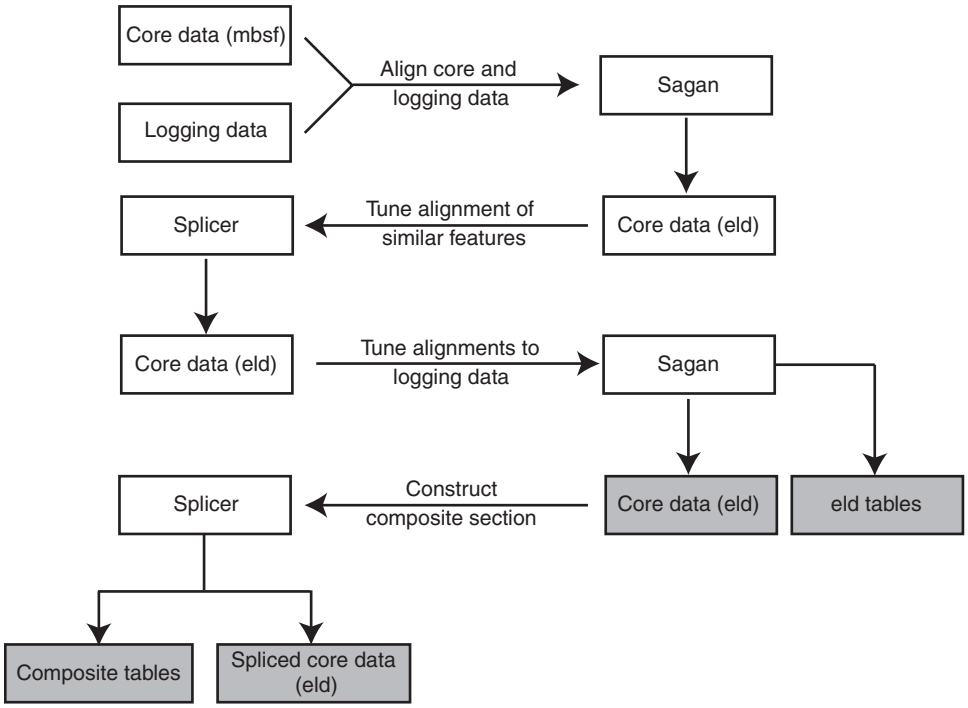

Figure F5. Comparison of the Hostile Environment Gamma Ray Sonde (HNGS), Multisensor Spectral Gamma Ray Tool (MGT), and Scintillation Gamma Ray Tool (SGT) data from the base of the black shale interval at Site 1260. Both the MGT and SGT provide data of comparable resolution, and higher than that acquired with the HNGS. However, the SGT provides data that extends deeper into the borehole, capturing (at Site 1260) the base of the black shale deposits at 486.5 equivalent logging depth (eld) below the base of the black shale interval. gAPI = American Petroleum Institute gamma ray units.

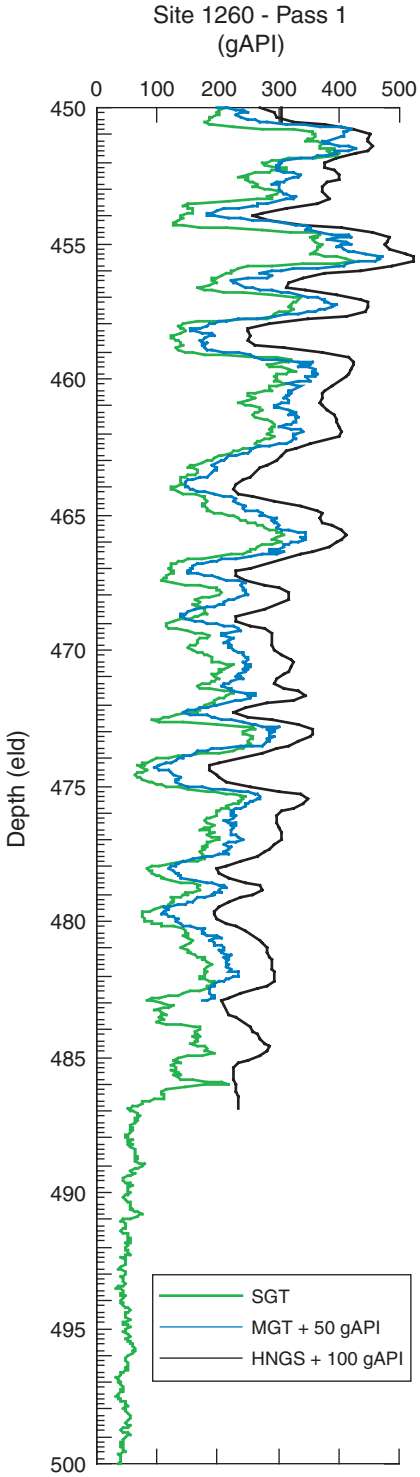

Figure F6. Detail of the depth-matched log and core data from the top of the black shale sequence at Site 1258. Logging at Site 1258 was performed in Hole 1258C. The top of the black shales in Hole 1258A, 1258B, and 1258C is not synchronous. Based upon the strong tie across all three holes at 402.92 equivalent logging depth (eld), the top of the black shale deposits in Hole 1258A extend over 2 m above the transition into the black shales identified in the logging data in Hole 1258C. Logging data (FMS pad averaged conductivity and Scintillation Gamma Ray Tool [SGT] natural gamma ray [NGR]) in red. cps = counts per second. gAPI = American Petroleum Institute gamma ray units.

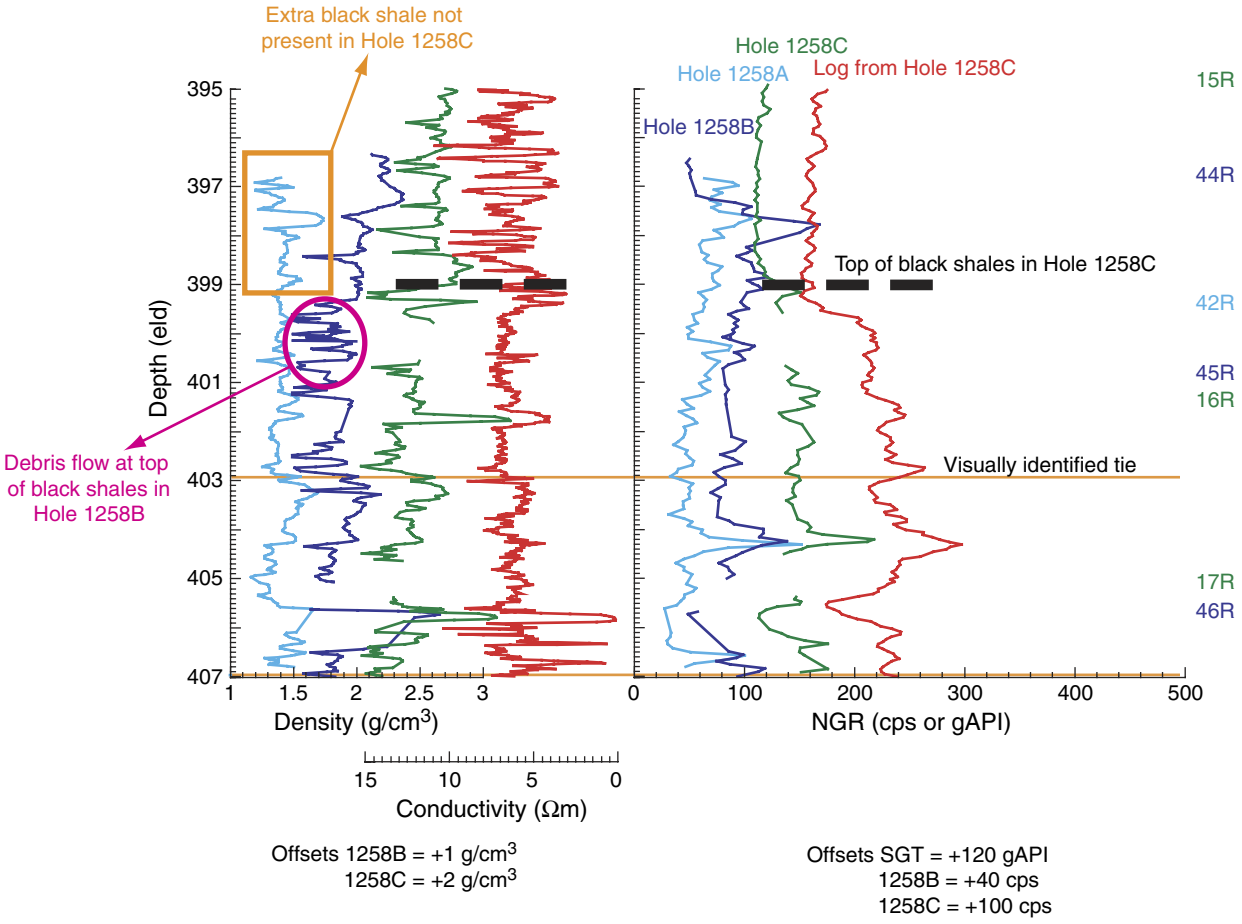

Figure F7. A. Log-integrated depths (equivalent logging depth [eld]) for MST density data from Holes 1258A (light blue), 1258B (dark blue), and 1258C (green). Core numbers are labeled with the same color scheme. Density has been integrated with pass 2 (red) of the FMS tool (pass 1 = gray). **B.** eld depths for Site 1258 displayed for the MST measurements of natural gamma ray (NGR) and the logging NGR recorded by the SGT. Depths of ties between the core and logging data are indicated by orange lines. **C.** Spliced record for density (blue) compared with the FMS data from pass 1 (gray) and pass 2 (red). Purple lines indicate position of tie points between the cores. Core numbers used in the splice are labeled. **D.** Spliced record for NGR (blue) compared with the SGT data from pass 1 (gray) and pass 2 (red). cps = counts per second. gAPI = American Petroleum Institute gamma ray units. (**Figure shown on next page.**)

Figure F7 (continued). (Caption shown on previous page.)

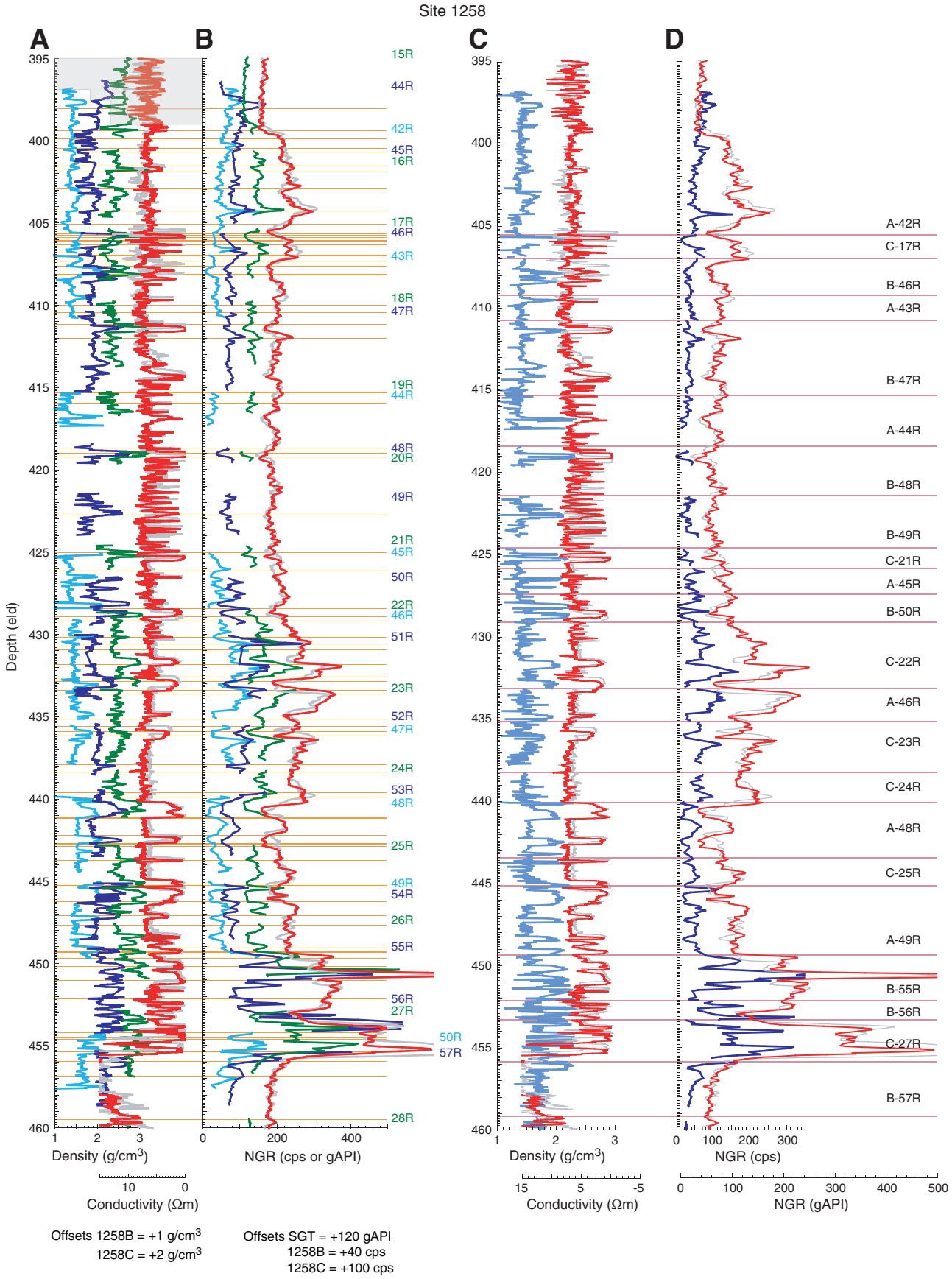

Figure F8. A. Log-integrated depths (equivalent logging depth [eld]) for MST density data from Holes 1260A (light blue) and 1260B (dark blue). Core numbers are labeled with the same color scheme. Density has been integrated with pass 1 (red) of the FMS tool (pass 2 = gray). **B.** eld depths for Site 1260 displayed for the MST measurements of natural gamma ray (NGR) and the logging NGR recorded by the SGT. Depths of ties between the core and logging data are indicated by orange lines. **C.** Spliced record for density (blue) compared with the FMS data from pass 1 (red) and pass 2 (gray). Purple lines indicate position of tie points between the cores. Core numbers used in the splice are labeled. **D.** Spliced record for NGR (blue) compared with the SGT data from pass 1 (red) and pass 2 (gray). cps = counts per second. gAPI = American Petroleum Institute gamma ray units. (**Figure shown on next page.**)

Figure F8 (continued). (Caption shown on previous page.)

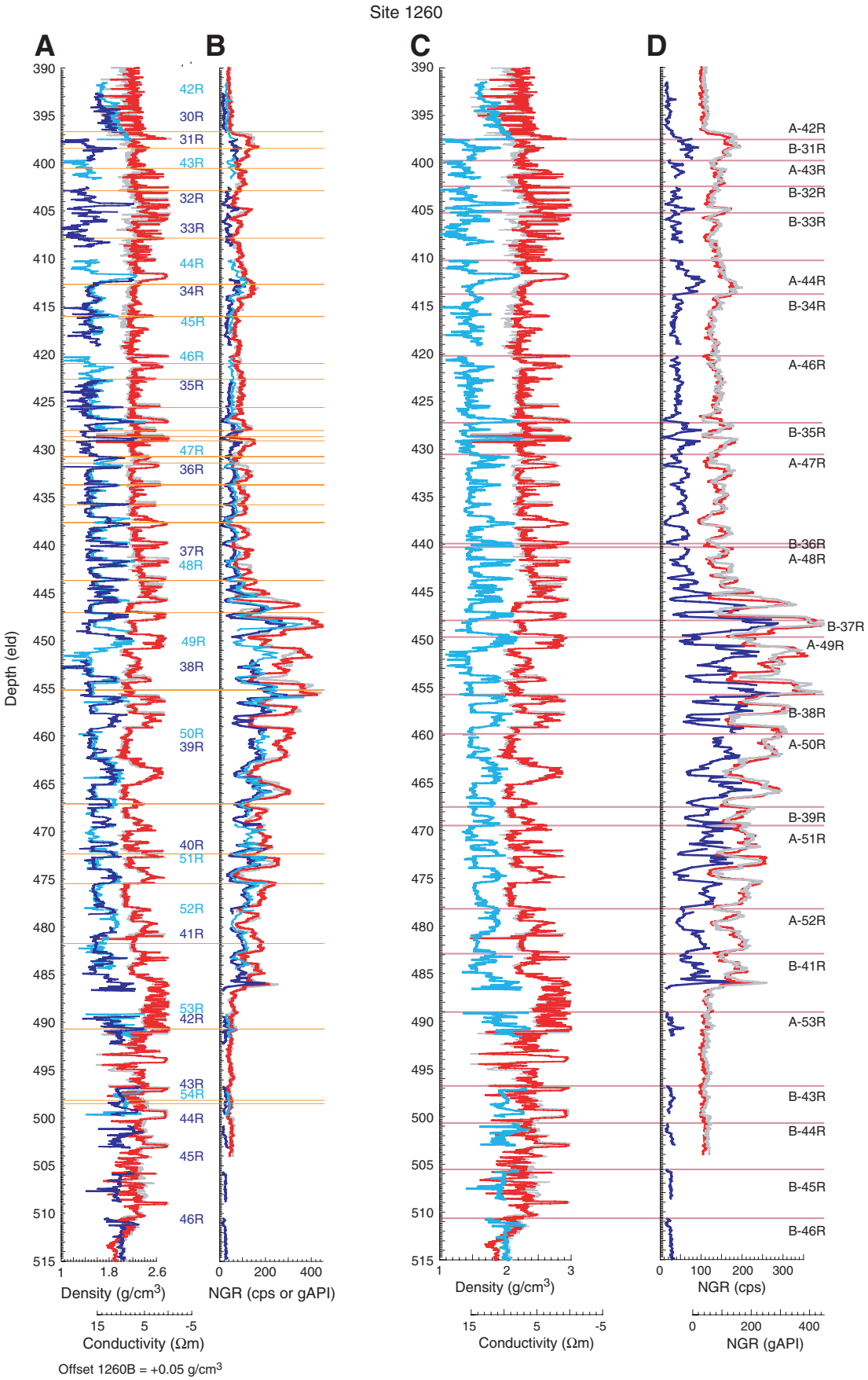

Figure F9. Detail of the depth-matched log and core data from the top of the black shale sequence at Site 1260. Logging data (FMS pad averaged conductivity and SGT natural gamma ray [NGR]) in red. eld = equivalent logging depth. cps = counts per second. gAPI = American Petroleum Institute gamma ray units.

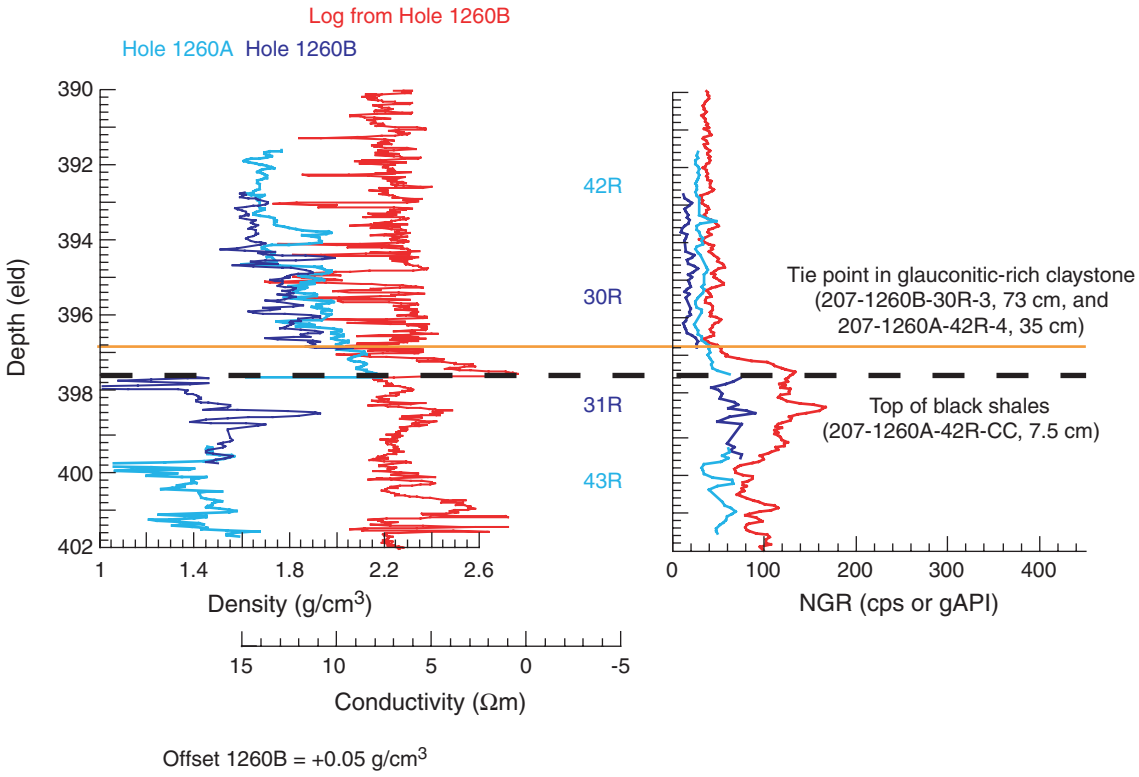

Figure F10. A. Log-integrated depths (equivalent logging depth [eld]) for MST density data from Holes 1261A (light blue) and 1261B (dark blue). Core numbers are labeled with the same color scheme. Density has been integrated with pass 1 (red) of the FMS tool (pass 2 = gray). **B.** eld depths for Site 1261 displayed for the MST measurements of natural gamma ray (NGR) and the logging NGR recorded by the SGT. Depths of ties between the core and logging data are indicated by orange lines. **C.** Spliced record for density (blue) compared with the FMS data from pass 1 (red) and pass 2 (gray). Purple lines indicate position of tie points between the cores. Core numbers used in the splice are labeled. **D.** Spliced record for NGR (blue) compared with the SGT data from pass 1 (red) and pass 2 (gray). cps = counts per second. gAPI = American Petroleum Institute gamma ray units. (**Figure shown on next page.**)

Figure F10 (continued). (Caption shown on previous page.)

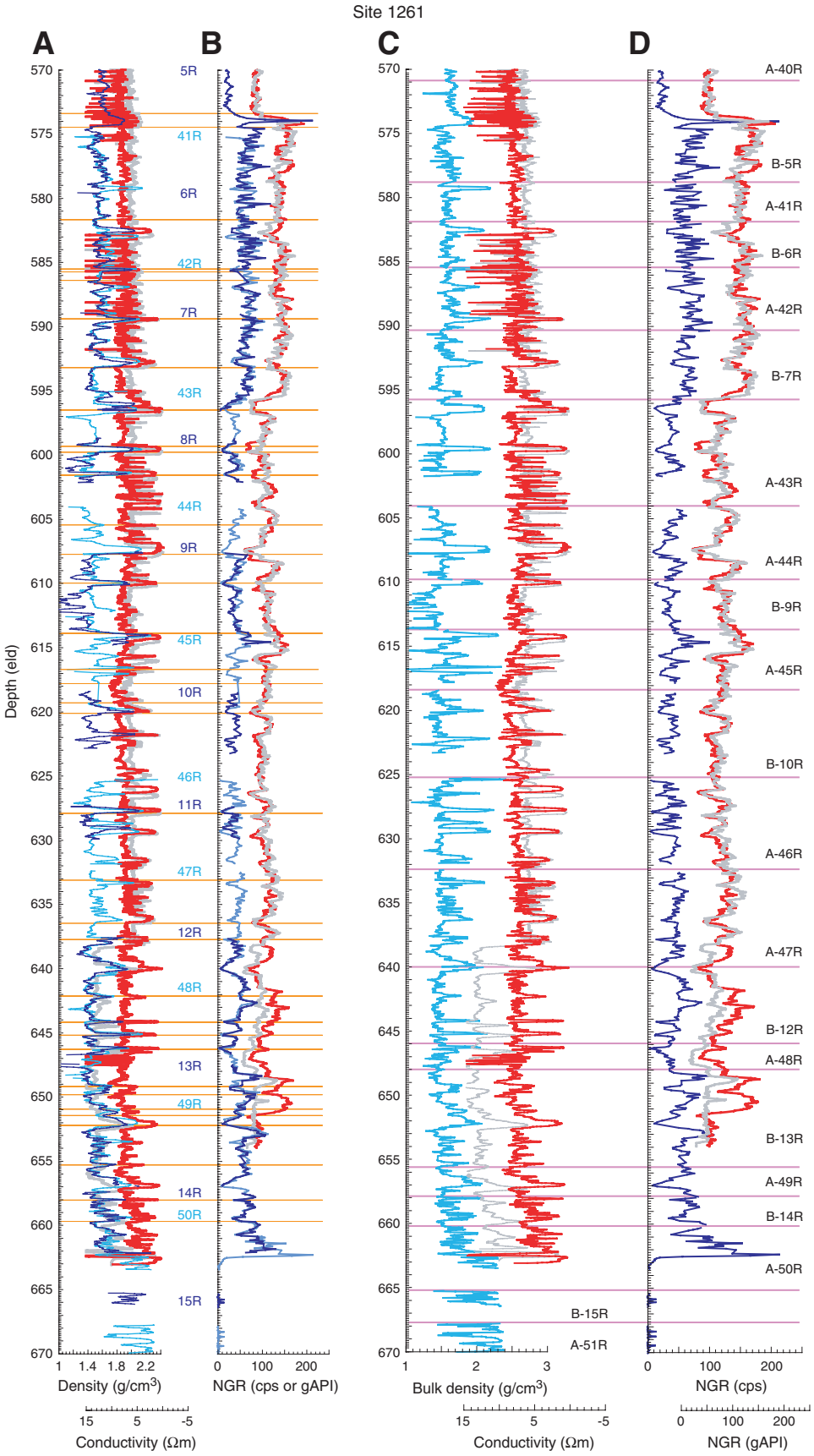

Figure F11. Detail of the depth-matched log and core data from the top of the black shale sequence at Site 1261. Logging data (FMS pad averaged conductivity and SGT natural gamma ray [NGR]) in red. eld = equivalent logging depth. cps = counts per second. gAPI = American Petroleum Institute gamma ray units.

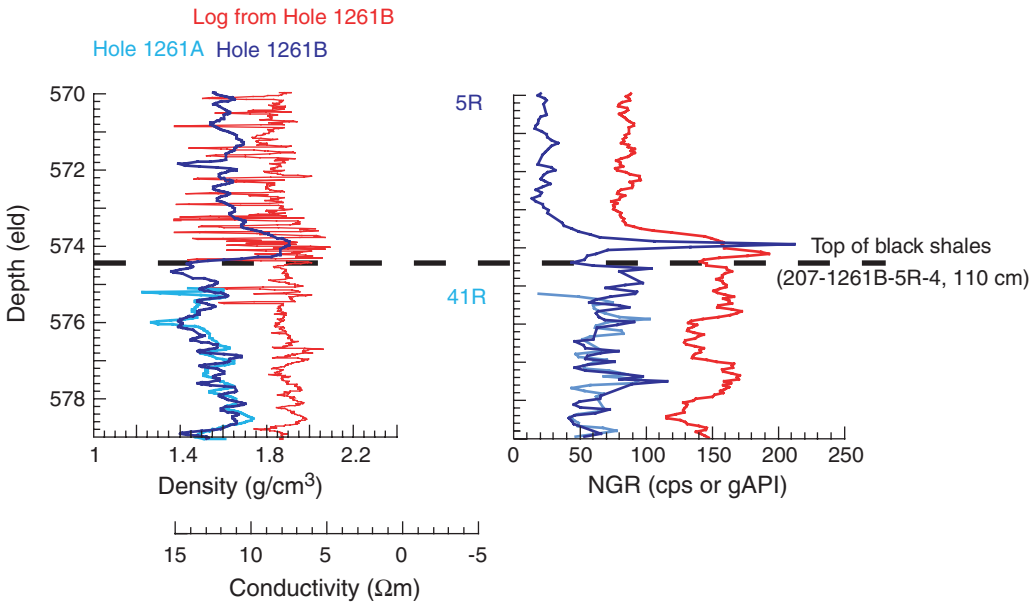

Table T1. Tie points used to correlate core (mbsf) depth scale with logging (equivalent logging depth [eld]) scale at Sites 1258, 1260, and 1261. (**See table notes.** Continued on next page.)

Core, section, interval (cm)	Depth (mbsf)	Depth (eld)	Compression (%)	Offset	Distance between tie points (mbsf)	Distance between tie points (eld)
207-1258A-						
40R-5, 48	376.98	383.92		6.94		
42R-1, 130	391.10	398.07	0.0	6.97	1.79	1.79
42R-3, 20	392.89	399.86	–1.7	6.97	0.60	0.61
42R-3, 80	393.49	400.47	–12.8	6.98	0.94	1.06
42R-4, 68	394.43	401.53	0.0	7.10	1.39	1.39
42R-5, 60	395.82	402.92	0.7	7.10	1.37	1.36
42R-6, 65	397.19	404.28	–4.0	7.09	0.75	0.78
42R-7, 0	397.94	405.06	6.3	7.12	0.63	0.59
42R-7, 63	398.57	405.65		7.08		
Intracore gap		0.45				
42R-7, 65	398.59	406.10		7.51		
43R-1, 118	400.58	408.13		7.55		
44R-1, 75	409.85	415.95		6.10		
45R-1, 110	419.80	426.18		6.38		
46R-1, 10	423.40	429.17	12.2	5.77	1.15	1.01
46R-1, 125	424.55	430.18	–6.9	5.63	4.67	4.99
46R-5, 50	429.22	435.17		5.95		
47R-1, 10	428.40	435.60		7.20		
47R-2, 90	430.70	437.90		7.20		
48R-1, 10	433.00	439.89	5.8	6.89	1.39	1.31
48R-2, 10	434.39	441.20	–32.1	6.81	0.78	1.03
48R-2, 88	435.17	442.23	–6.0	7.06	0.50	0.53
48R-2, 138	435.67	442.76	–94.0	7.09	0.50	0.97
48R-3, 38	436.17	443.73		7.56		
49R-1, 38	438.27	445.28	–28.0	7.01	0.75	0.96
49R-1, 113	439.02	446.24	0.7	7.22	2.87	2.85
49R-3, 105	441.89	449.09		7.20		
Intracore gap		0.24				
49R-3, 108	441.92	449.33	0.0	7.41	0.37	0.37
49R-3, 145	442.29	449.70		7.41		
50R-1, 8	442.58	454.22	–8.1	11.64	0.37	0.40
50R-1, 45	442.95	454.62	19.8	11.67	0.96	0.77
50R-2, 15	443.91	455.39		11.48		
207-1258B-						
44R-2, 110	395.26	398.07		2.81		
45R-1, 70	398.20	400.47	–32.5	2.27	0.80	1.06
45R-2, 50	399.00	401.53	–18.8	2.53	1.17	1.39
45R-3, 83	400.17	402.92	–11.5	2.75	1.22	1.36
45R-4, 63	401.39	404.28	–1.3	2.89	0.77	0.78
45R-4, 140	402.16	405.06		2.90		
46R-1, 23	403.33	405.73	–51.2	2.40	0.41	0.62
46R-2, 0	403.74	406.35	6.2	2.61	0.65	0.61
46R-2, 65	404.39	406.96	–85.7	2.57	0.35	0.65
46R-2, 100	404.74	407.61	37.9	2.87	0.87	0.54
46R-3, 38	405.61	408.15	0.0	2.54	1.86	1.86
46R-4, 125	407.47	410.01		2.54		
47R-1, 10	407.20	410.45	–0.6	3.25	1.54	1.55
47R-2, 45	408.74	412.00	0.6	3.26	3.30	3.28
47R-4, 100	412.04	415.28		3.24		
48R-1, 10	412.80	418.66	2.9	5.86	0.35	0.34
48R-1, 45	413.15	419.00		5.85		
49R-2, 50	418.70	422.76		4.06		
50R-2, 43	424.17	428.41		4.24		
51R-1, 130	427.60	430.95	–109.5	3.35	0.42	0.88
51R-2, 30	428.02	431.83	–5.1	3.81	0.99	1.04
51R-3, 5	429.01	432.87	34.7	3.86	1.18	0.77
51R-4, 15	430.19	433.64		3.45		
52R-1, 75	432.65	436.18		3.53		
53R-1, 20	436.10	439.63	3.9	3.53	1.55	1.49
53R-2, 55	437.65	441.12	–97.5	3.47	0.80	1.58
53R-2, 135	438.45	442.70		4.25		
54R-1, 10	441.60	445.18		3.58		
55R-1, 30	445.80	449.30	–32.4	3.50	0.68	0.90
55R-1, 98	446.48	450.20	7.9	3.72	0.89	0.82
55R-2, 75	447.37	451.02	29.7	3.65	1.58	1.11
55R-4, 38	448.95	452.13		3.18		
56R-1, 15	451.35	452.13		0.78		
57R-1, 83	456.02	455.97		–0.05		
207-1258C-						
14R-3, 18	387.88	392.52		4.64		
15R-3, 125	394.02	399.38		5.36		
16R-1, 10	394.50	400.70	1.7	6.20	1.20	1.18
16R-1, 130	395.70	401.88	–18.2	6.18	0.88	1.04
16R-2, 68	396.58	402.92	–8.8	6.34	1.25	1.36
16R-3, 53	397.83	404.28		6.45		
17R-1, 48	399.88	405.68	0.0	5.80	0.20	0.20
17R-1, 68	400.08	405.88		5.80		
Intracore gap		0.19				
17R-1, 70	400.10	406.07	–1.1	5.97	0.92	0.93
17R-2, 23	401.02	407.00		5.98		
Intracore gap		0.30				
17R-2, 25	401.04	407.30		6.26		
18R-2, 48	405.89	411.18		5.29		
19R-1, 10	409.20	415.33		6.13		
20R-1, 40	414.10	419.22		5.12		
21R-1, 40	419.10	425.02		5.92		
22R-1, 50	423.80	428.93	–5.7	5.13	1.58	1.67
22R-2, 95	425.38	430.60	–3.1	5.22	1.93	1.99
22R-4, 65	427.31	432.59		5.28		
23R-1, 10	428.40	433.42	–15.7	5.02	2.17	2.51
23R-2, 100	430.57	435.93		5.36		
24R-1, 10	433.00	438.36		5.36		
25R-1, 10	438.00	442.88	–13.3	4.88	0.75	0.85
25R-1, 85	438.75	443.73	–6.7	4.98	3.14	3.35
25R-3, 108	441.89	447.08		5.19		
26R-1, 10	442.60	447.66		5.06		
27R-2, 23	449.14	454.52	0.0	5.38	2.34	2.34
27R-3, 108	451.48	456.86		5.38		
28R-1, 10	451.90	459.51		7.61		
30R-1, 10	461.50	467.57		6.07		
31R-1, 10	466.50	472.19		5.69		
207-1260A-						
42R-4, 35	389.35	396.50		7.15		
43R-2, 35	395.73	400.74		5.01		
44R-2, 120.5	406.41	412.68		6.27		
45R-1, 110	409.80	416.06		6.26		
46R-1, 82.5	415.12	420.97	6.2	5.85	1.76	1.65
46R-2, 132.5	416.88	422.62	–6.1	5.74	2.79	2.96
46R-4, 138.5	419.67	425.58		5.91		
47R-1, 12.5	424.02	430.73	–34.6	6.71	0.50	0.67
47R-1, 62.5	424.52	431.40	–6.0	6.88	2.18	2.31
47R-2, 130	426.70	433.71	3.7	7.01	2.15	2.07
47R-4, 45	428.85	435.78	7.1	6.93	2.01	1.87
47R-5, 97.5	430.86	437.65		6.79		
48R-3, 22.5	436.62	443.70	3.9	7.08	3.53	3.39
48R-5, 97.5	440.15	447.10		6.95		
49R-4, 104.5	448.49	455.20		6.71		
50R-6, 25	460.45	467.10		6.65		
51R-3, 64.5	465.62	472.36	–4.8	6.74	2.98	3.12
51R-5, 62	468.60	475.48		6.88		
52R-3, 27.5	474.85	481.73		6.88		
53R-2, 15	482.95	490.69		7.74		
54R-2, 37.5	489.77	498.51		8.74		
207-1260B-						
30R-3, 73	390.23	396.50		6.27		
31R-1, 100	392.10	398.51		6.41		
32R-1, 5	396.15	402.85	0.8	6.70	1.69	1.68
32R-2, 30	397.84	404.53		6.69		
33R-2, 142.5	403.62	407.87		4.25		
34R-1, 102.5	406.73	412.68	3.5	5.95	3.50	3.38

Table T1 (continued).

Core, section, interval (cm)	Depth (mbsf)	Depth (eld)	Compression (%)	Offset	Distance between tie points (mbsf)	Distance between tie points (eld)
34R-4, 3	410.23	416.06		5.83		
35R-2, 142.5	418.23	425.58	–1.5	7.35	2.39	2.43
35R-4, 85	420.62	428.01	–13.1	7.39	0.55	0.62
35R-4, 140	421.17	428.63	–58.8	7.46	0.28	0.44
35R-5, 17.5	421.45	429.07	16.6	7.62	1.98	1.65
35R-6, 66.5	423.43	430.73		7.30		
36R-2, 55	426.95	433.71	3.7	6.76	2.15	2.07
36R-3, 120	429.10	435.78	7.1	6.68	2.01	1.87
36R-5, 20.5	431.11	437.65		6.54		
37R-3, 33.5	437.84	443.70		5.86		
38R-3, 22.5	447.33	455.20		7.87		
39R-5, 90	460.60	467.10		6.50		
40R-2, 12.5	464.73	472.36	–5.2	7.63	2.97	3.12
40R-4, 10	467.70	475.48		7.78		
41R-2, 22.5	474.42	481.73		7.31		
42R-2, 15	483.73	490.69		6.96		
43R-1, 122.5	489.12	498.17		9.05		
207-1261A-						
41R-5, 54.5	570.35	581.65	–0.2	11.30	0.95	0.95
41R-5, 150	571.30	582.61		11.31		
42R-1, 40	573.80	585.54	–7.0	11.74	3.61	3.86
42R-3, 113.5	577.41	589.40	–4.5	11.99	3.61	3.77
42R-6, 25.5	581.02	593.17		12.15		
43R-2, 2	584.52	596.50	–43.9	11.98	1.95	2.81
43R-3, 50	586.47	599.31	–1.6	12.84	0.45	0.46
43R-3, 95	586.92	599.76	36.5	12.84	2.86	1.82
43R-5, 92.5	589.78	601.58		11.80		
44R-1, 130	593.90	605.44	9.7	11.54	0.90	0.81
44R-2, 70	594.80	606.25	–39.2	11.45	1.04	1.45
44R-3, 47.5	595.84	607.70	6.5	11.86	2.43	2.27
44R-4, 142.5	598.27	609.97		11.70		
45R-1, 122	603.42	613.87	10.3	10.45	2.04	1.83
45R-3, 47.5	605.46	615.70	–28.7	10.24	0.70	0.90
45R-3, 117.5	606.16	616.60	–4.7	10.44	1.14	1.19
45R-4, 80	607.30	617.80		10.50		
Intracore gap		1.50				
45R-4, 82.5	607.33	619.30		11.97		
46R-3, 42.5	615.09	627.89	32.1	12.80	2.15	1.46
46R-4, 107.5	617.24	629.35	–56.9	12.11	1.40	2.20
46R-5, 100	618.64	631.55		12.91		
47R-1, 72.5	622.12	633.10	2.5	10.98	3.45	3.37
47R-3, 135	625.57	636.47	5.0	10.90	1.35	1.28
47R-4, 120	626.92	637.75		10.83		
48R-1, 105	632.05	642.13	4.9	10.08	2.15	2.04
48R-3, 20	634.20	644.18	–27.0	9.97	0.80	1.02
48R-3, 100.5	635.00	645.19	14.7	10.19	1.28	1.09
48R-4, 77.5	636.28	646.28	–2.1	10.00	2.85	2.91
48R-6, 68.5	639.13	649.19		10.06		
49R-1, 79	641.39	650.94	–33.8	9.55	0.37	0.50
49R-1, 116.5	641.76	651.44	–64.9	9.68	0.47	0.78
49R-2, 15	642.23	652.21	9.5	9.98	3.41	3.09
49R-4, 56.5	645.64	655.30	3.2	9.66	2.82	2.73
49R-6, 37.5	648.46	658.03		9.57		
50R-1, 60	650.80	659.69	0.4	8.89	2.45	2.44
50R-3, 5	653.25	662.13		8.88		
207-1261B-						
5R-4, 15	562.36	573.39	–8.0	11.03	1.00	1.08
5R-4, 115	563.36	574.47		11.11		
6R-2, 62	570.52	581.65	–0.2	11.13	0.95	0.95
6R-3, 7	571.47	582.61	26.3	11.14	3.93	2.90
6R-5, 100	575.40	585.50	–14.5	10.10	0.20	0.23
6R-5, 120	575.60	585.73		10.13		
Intracore gap		0.67				
6R-5, 122.5	575.62	586.40		10.78		
7R-1, 45	578.45	589.40	–4.5	10.95	3.61	3.77
7R-3, 108	582.06	593.17	–5.9	11.11	1.87	1.98
7R-4, 145	583.93	595.15	14.3	11.22	1.57	1.35
7R-6, 50	585.50	596.50		11.00		
8R-1, 53.5	588.13	599.31	–1.6	11.18	0.45	0.46
8R-1, 97.5	588.58	599.76	4.9	11.18	1.87	1.78
8R-2, 135	590.45	601.54		11.09		
9R-1, 25	597.45	607.74	–38.8	10.29	1.61	2.24
9R-2, 36	599.06	609.97	–4.5	10.91	3.73	3.90
9R-4, 113.5	602.79	613.87		11.08		
10R-2, 32.5	608.62	620.11	0.3	11.49	1.96	1.95
10R-3, 77.5	610.58	622.06		11.48		
12R-1, 22.5	626.22	637.75	–2.4	11.53	4.28	4.38
12R-4, 5	630.50	642.13	4.9	11.63	2.15	2.04
12R-5, 70.5	632.65	644.18	–27.0	11.53	0.80	1.02
12R-6, 20	633.45	645.19	14.7	11.74	1.28	1.09
12R-6, 148	634.73	646.28		11.55		
13R-2, 27.5	637.38	649.19	5.2	11.81	0.67	0.63
13R-2, 95	638.05	649.83	–2.5	11.78	1.09	1.12
13R-3, 57.5	639.14	650.94	–33.8	11.80	0.37	0.50
13R-3, 95	639.51	651.44	–64.9	11.93	0.47	0.78
13R-3, 142	639.98	652.21	9.5	12.23	3.41	3.09
13R-6, 32.5	643.39	655.30		11.91		
14R-1, 67.5	645.88	658.03	6.3	12.15	1.89	1.66
14R-2, 107	647.77	659.69		11.92		

Notes: Ties are mapped across all holes when multiple copies of an interval were determined to occur at a given depth. Where more than one tie exists within a core, the compression required to correct the mbsf sampling interval to the eld scale is calculated. Negative compression indicates that stretching of the interval is required.

Table T2. Reported depths to seafloor as recorded by the drillers, loggers, and the background/operations summary.

	Drillers (mbrf)	Operations (mbsl)	Loggers (mbrf)
Site 1258	3203	3192	3195
Site 1260	2560	2549	2553
Site 1261	1911	1899	1899

Note: Depths reported for the operations come from the 3.5-kHz recorder, and although they approximate the loggers depths, are reported in mbsl, not mbrf.

Table T3. Composite section tie points for Site 1258 log-adjusted coring data.

Hole, core, section, interval (cm)	Depth (mbsf)	Depth (eld)		Hole, core, section, interval (cm)	Depth (mbsf)	Depth (eld)	Break in record (m)
207-				207-			
1258A-42R-7, 50	398.49	405.53	Tie to	1258C-17R-1, 26	399.71	405.53	
1258C-17R-2, 20	401.04	406.97	Tie to	1258B-46R-2, 61.5	404.41	406.97	
1258B-46R-4, 42.5	406.70	409.19	Tie to	1258A-43R-2, 114.5	401.88	409.19	
1258A-43R-4, 67.5	403.72	410.73	Tie to	1258B-47R-1, 37.5	407.53	410.73	
1258B-47R-4, 100	412.09	415.28	Append to	1258A-44R-1, 0	409.15	415.31	0.03
1258A-44R-2, 87.5	411.27	417.36	Append to	1258B-48R-1, 0	412.75	418.39	1.03
1258B-48R-1, 137.5	414.13	419.63	Append to	1258B-49R-1, 0	416.75	421.39	1.76
1258B-49R-3, 50	419.92	423.97	Append to	1258C-21R-1, 0	418.75	424.56	0.59
1258C-21R-2, 12.5	420.13	425.83	Tie to	1258A-45R-1, 76	419.51	425.83	
1258A-45R-2, 127.5	421.31	427.39	Tie to	1258B-50R-1, 87	423.22	427.39	
1258B-50R-3, 15	425.17	429.11	Tie to	1258C-22R-1, 66	424.01	429.11	
1258C-22R-4, 137.5	428.09	433.14	Tie to	1258A-46R-3, 150	427.67	433.14	
1258A-46R-5, 50	429.27	435.17	Tie to	1258C-23R-2, 33.5	429.96	435.17	
1258C-23R-3, 142.5	432.49	437.79	Append to	1258C-24R-1, 0	432.95	438.26	0.47
1258C-24R-2, 57.5	434.95	440.07	Tie to	1258A-48R-1, 28.5	433.24	440.07	
1258A-48R-3, 22.5	436.07	443.44	Tie to	1258C-25R-1, 60	438.55	443.44	
1258C-25R-2, 72.5	440.13	445.14	Tie to	1258A-49R-1, 18.5	438.14	445.14	
1258A-49R-3, 112.5	442.02	449.37	Tie to	1258B-55R-1, 35	445.90	449.37	
1258B-55R-4, 45	449.07	452.13	Tie to	1258B-56R-1, 5	451.30	452.13	
1258B-56R-2, 52.5	452.85	453.32	Tie to	1258C-27R-1, 48.5	448.04	453.32	
1258C-27R-3, 5	450.51	455.84	Tie to	1258B-57R-1, 66	455.91	455.84	
1258B-57R-3, 50	458.75	458.65	Append to	1258C-28R-1, 0	451.85	459.15	0.50
1258C-28R-2, 82.5	454.18	461.38	Append to	1258C-29R-1, 0	456.85	463.62	2.24
1258C-29R-3, 82.5	460.68	466.83	Append to	1258C-30R-1, 0	461.45	467.47	0.64
1258C-30R-3, 125	465.42	471.14	Append to	1258C-31R-1, 0	466.45	472.09	0.95
1258C-31R-3, 50	469.95	475.59	Append to	1258C-32R-1, 0	471.05	476.69	1.10
1258C-32R-2, 95	473.37	479.01	Append to	1258C-33R-1, 0	476.05	481.69	2.68
1258C-33R-3, 70	479.75	485.39	Append to	1258C-34R-1, 0	480.75	486.39	1.00
1258C-34R-3, 110	484.85	490.49					
					Total missing (m):		3.88
					Total cored (m):		53.12
					% recovery:		93.19

Notes: eld = equivalent logging depth. Gaps in the composite record are highlighted and the amount of compression needed to adjust intervals between ties within the same core calculated. Compression (%) = (Δmbsf/Δeld) $\times$ 100.

Table T4. Composite section tie points for Site 1260 log-adjusted coring data.

Hole, core, section, interval (cm)	Depth (mbsf)	Depth (eld)		Hole, core, section, interval (cm)	Depth (mbsf)	Depth (eld)	Break in record (m)
207-				207-			
1260A-42R-4, 138	390.38	397.52	Tie to	1260B-31R-1, 0	391.10	397.52	
1260B-31R-2, 37.5	392.98	399.36	Tie to	1260A-43R-1, 21	394.31	399.36	
1260A-43R-2, 105	396.43	401.44	Append to	1260B-32R-1, 0	396.10	402.80	1.36
1260B-32R-2, 87.5	398.42	405.08	Tie to	1260B-33R-1, 5	400.12	405.08	
1260B-33R-3, 70	404.40	408.67	Append to	1260A-44R-1, 0	403.70	409.98	1.31
1260A-44R-4, 15	407.65	413.88	Tie to	1260B-34R-2, 77.5	407.98	413.88	
1260B-34R-6, 60	413.30	419.12	Append to	1260A-46R-1, 0	414.30	420.16	1.04
1260A-46R-6, 20	421.27	427.16	Tie to	1260B-35R-3, 151	419.81	427.16	
1260B-35R-6, 60	423.37	430.68	Tie to	1260A-47R-1, 7.5	423.98	430.68	
1260A-47R-7, 82.5	432.95	439.79	Tie to	1260B-36R-6, 80	433.20	439.79	
1260B-36R-6, 122.5	433.62	440.22	Append to	1260A-48R-1, 0	433.50	440.51	0.29
1260A-48R-6, 37.5	441.05	448.02	Tie to	1260B-37R-6, 15	442.15	448.02	
1260B-37R-7, 42.5	443.92	449.80	Tie to	1260A-49R-1, 10	443.20	449.80	
1260A-49R-5, 15	449.10	455.80	Tie to	1260B-38R-3, 83.5	447.93	455.80	
1260B-38R-6, 52.5	451.98	459.81	Tie to	1260A-50R-1, 38.5	453.09	459.81	
1260A-50R-6, 42.5	460.62	467.26	Tie to	1260B-39R-5, 107	460.77	467.26	
1260B-39R-7, 55	463.25	469.48	Tie to	1260A-51R-1, 42.5	462.42	469.48	
1260A-51R-7, 60	471.16	478.26	Tie to	1260A-52R-1, 5	471.65	478.26	
1260A-52R-3, 145	476.03	482.94	Tie to	1260B-41R-2, 140	475.60	482.94	
1260B-41R-5, 60	479.24	486.66	Append to	1260A-53R-1, 0	481.30	489.01	2.35
1260A-53R-2, 50	483.30	491.10	Tie to	1260B-42R-2, 48.5	484.06	491.10	
1260B-42R-3, 65	485.62	492.95	Append to	1260B-43R-1, 0	487.90	496.73	3.78
1260B-43R-3, 47.5	491.12	500.18	Append to	1260B-44R-1, 0	491.90	500.87	0.69
1260B-44R-2, 75	494.12	503.09	Append to	1260B-45R-1, 0	496.50	505.47	2.38
1260B-45R-2, 147.5	499.48	508.45	Append to	1260B-46R-1, 0	501.50	510.47	2.02
1260B-46R-4, 100	507.00	515.97					
					Total missing (m):		4.00
					Total cored (m):		85.42
					% recovery:		95.53

Notes: eld = equivalent logging depth. Gaps in the composite record are highlighted and the amount of compression needed to adjust intervals between ties within the same core calculated. Compression (%) = (Δmbsf/Δeld) $\times$ 100.

Table T5. Composite section tie points for Site 1261 log-adjusted coring data.

Hole, core, section, interval (cm)	Depth (mbsf)	Depth (eld)		Hole, core, section, interval (cm)	Depth (mbsf)	Depth (eld)	Break in record (m)
207-				207-			
1261A-40R-5, 32.5	560.54	570.89	Tie to	1261B-5R-2, 47	559.90	570.89	
1261B-5R-8, 5	567.81	578.81	Tie to	1261A-41R-3, 69.5	567.55	578.81	
1261A-41R-5, 80	570.65	581.90	Tie to	1261B-6R-2, 86	570.81	581.90	
1261B-6R-5, 95	575.40	585.46	Tie to	1261A-42R-1, 31	573.76	585.46	
1261A-42R-4, 55	578.37	590.35	Tie to	1261B-7R-1, 134.5	579.40	590.35	
1261B-7R-5, 65	584.68	595.75	Tie to	1261A-43R-1, 75	583.80	595.75	
1261A-43R-5, 107.5	589.98	601.73	Append to	1261A-44R-1, 0	592.65	604.05	2.32
1261A-44R-4, 122.5	598.12	609.79	Tie to	1261B-9R-2, 20.5	598.96	609.79	
1261B-9R-4, 97.5	602.68	613.70	Tie to	1261A-45R-1, 105	603.30	613.70	
1261A-45R-4, 80	607.35	617.80	Append to	1261B-10R-1, 0	606.85	618.39	0.59
1261B-10R-3, 140	611.25	623.29	Append to	1261A-46R-1, 0	611.85	625.22	1.93
1261A-46R-5, 135	619.04	631.90	Append to	1261A-47R-1, 0	621.45	632.39	0.49
1261A-47R-6, 45	629.17	640.00	Tie to	1261B-12R-2, 97.5	628.48	640.00	
1261B-12R-6, 110	634.40	645.96	Tie to	1261A-48R-4, 40	635.95	645.96	
1261A-48R-5, 100	638.00	647.99	Tie to	1261B-13R-1, 60	636.25	647.99	
1261B-13R-6, 65	643.76	655.61	Tie to	1261A-49R-4, 87.5	646.01	655.61	
1261A-49R-6, 20	648.33	657.86	Tie to	1261B-14R-1, 50	645.75	657.86	
1261B-14R-3, 7.5	648.33	660.20	Tie to	1261A-50R-1, 109.5	651.35	660.20	
1261A-50R-3, 140	654.65	663.49	Append to	1261B-15R-1, 0	654.85	665.20	1.71
1261B-15R-1, 125	656.10	666.45	Append to	1261A-51R-1, 0	659.85	667.72	1.27
1261A-51R-2, 107.5	662.25	670.12	Append to	1261B-16R-1, 0	664.55	674.90	4.78
1261B-16R-1, 142.5	665.98	676.32					
						Total missing (m):	5.33
						Total cored (m):	92.60
						% recovery:	94.56

Notes: eld = equivalent logging depth. Gaps in the composite record are highlighted and the amount of compression needed to adjust intervals between ties within the same core calculated. Compression (%) = (Δmbsf/Δeld) $\times$ 100.